Substitution Chemistry of Carbonyl and Sulphur Dioxide *triangulo*-Platinum Clusters. Crystal Structure of $[Pt_3(\mu\text{-}CO)(\mu\text{-}SO_2)_2\{P(C_6H_{11})_3\}_3]$ †

Simon G. Bott, Andrew D. Burrows, Osayi J. Ezomo, Malcolm F. Hallam, John G. Jeffrey, and D. Michael P. Mingos*

Inorganic Chemistry Laboratory, University of Oxford, South Parks Road, Oxford OX1 3QR

The simple substitution chemistry of the *triangulo*-platinum clusters $[Pt_3(\mu\text{-}CO)_{3-n}(\mu\text{-}SO_2)_n\{P(C_6H_{11})_3\}_3]$ (n = 0—3) with carbon monoxide and sulphur dioxide ligands is described and some mechanistic implications discussed. Different products were isolated depending on the concentration of the gaseous reactants. For example, when 1 molar equivalent of carbon monoxide was added to $[Pt_3(\mu\text{-}SO_2)_3\{P(C_6H_{11})_3\}_3]$ (**1**) the monosubstituted carbon monoxide complex $[Pt_3(\mu\text{-}CO)(\mu\text{-}SO_2)_2\{P(C_6H_{11})_3\}_3]$ (**2**) was formed. However, with excess of carbon monoxide, using dichloromethane as the solvent, a relatively unstable dimer, $[Pt_2(\mu\text{-}SO_2)(CO)_2\{P(C_6H_{11})_3\}_2]$ (**3**) was isolated. This dimer was also prepared by the reaction of SO_2 with $[Pt_3(\mu\text{-}CO)_3\{P(C_6H_{11})_3\}_3]$ (**5**). With benzene as the solvent, compound (**1**) reacts with excess of CO to give the disubstituted cluster $[Pt_3(\mu\text{-}CO)_2(\mu\text{-}SO_2)\{P(C_6H_{11})_3\}_3]$ (**4**). The molecular structure of (**2**) has been determined by a single-crystal *X*-ray diffraction study. It crystallises in monoclinic space group *C*2/*m*, with four units of formula $[Pt_3(\mu\text{-}CO)(\mu\text{-}SO_2)_2\{P(C_6H_{11})_3\}_3]\cdot 0.5C_6H_6$ in a cell of dimensions of a = 24.909(9), b = 21.694(4), c = 15.559(4) Å, and β = 125.41(3)°. The structure consists of an isosceles triangle of Pt atoms with Pt–Pt distances of 2.678(1) and 2.710(1) Å. The Pt–Pt edges bridged by the sulphur dioxide ligands are appreciably longer than that bridged by carbon monoxide. The substitution chemistry of the mixed substituted clusters, (**2**) and (**4**) with xylyl isocyanide has been studied. The reactivities of both clusters resemble that of (**1**).

The *triangulo*-platinum cluster compounds $[Pt_3(\mu\text{-}X)_3(PR_3)_3]$ (X = CO or SO_2) have attracted considerable attention recently.[1–4] They have been used as precursors for heterometallic tetrahedral,[5] trigonal-bipyramidal,[6] and sandwich[7] cluster compounds, and their reactions with small unsaturated molecules and phosphines have been investigated.[2,8] Ligand-substitution reactions with phosphines occur rapidly and are thought to proceed through 44-electron intermediates in the manner shown in Scheme 1.

$$[Pt_3(\mu\text{-}CO)_3(PR_3)_3] + PR'_3 \longrightarrow [Pt_3(\mu\text{-}CO)_3(PR_3)_3(PR'_3)]$$

$$\downarrow -PR_3$$

$$[Pt_3(\mu\text{-}CO)_3(PR_3)_2(PR'_3)],\ etc.$$

Scheme 1.

Circumstantial evidence for these intermediates comes from *X*-ray crystallographic analyses on $[Pt_3(\mu\text{-}CO)_3\{P(C_6H_{11})_3\}_4]$[9] and $[Pt_3(\mu\text{-}SO_2)_3\{P(C_6H_{11})_3\}_2\{(Ph_2P)_2C_3H_6\}]$.[10] The substitution reactions involving unsaturated ligands such as CO, SO_2, and CNC_8H_9 (2,6-dimethylxylyl isocyanide) are more complex and can lead to cluster fragmentation and, with isocyanides, phosphine replacement. For example, although $[Pt_3(\mu\text{-}CO)_3\{P(C_6H_{11})_3\}_3]$ can be transformed in high yield into $[Pt_3(\mu\text{-}SO_2)_3\{P(C_6H_{11})_3\}_3]$, Farrar and co-workers[8] have noted that the related reaction with $[Pt_3(\mu\text{-}CO)_3(PBu^t{}_2Ph)_3]$ results in the formation of $[Pt_2(\mu\text{-}SO_2)(CO)_2(PBu^t{}_2Ph)_2]$. The reaction of $[Pt_3(\mu\text{-}CO)_3\{P(C_6H_{11})_3\}_3]$ with 3 and 5 equivalents of CNC_8H_9 results in the retention of the metal triangle, but occurs with phosphine replacement. The products of these reactions are $[Pt_3(\mu\text{-}CO)(\mu\text{-}CNC_8H_9)_2(CNC_8H_9)\{P(C_6H_{11})_3\}_2]$ and $[Pt_3(\mu\text{-}CN\text{-}C_8H_9)_3(CNC_8H_9)_2\{P(C_6H_{11})_3\}]$ respectively.[2] In order to shed further light on these reactions we have synthesised the complete range of *triangulo*-cluster compounds $[Pt_3(\mu\text{-}CO)_{3-n}(\mu\text{-}SO_2)_n\{P(C_6H_{11})_3\}_3]$ (n = 0—3) and studied their reactions with CNC_8H_9.

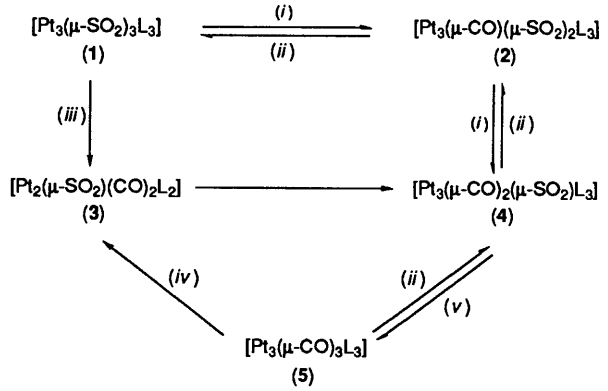

Scheme 2. L = $P(C_6H_{11})_3$. (*i*) 1 equivalent of CO; (*ii*) 1 equivalent of SO_2; (*iii*) CO, CH_2Cl_2; (*iv*) SO_2; (*v*) excess of CO, Me_3NO

Results and Discussion

It has proved possible to isolate the whole range of *triangulo*-clusters $[Pt_3(\mu\text{-}CO)_{3-n}(\mu\text{-}SO_2)_n\{P(C_6H_{11})_3\}_3]$ (n = 0—3) by varying the reaction conditions and the stoicheiometry. The transformations are summarised in Scheme 2, and where the

† μ-Carbonyl-1:2κ²*C*-di-μ-sulphur dioxide-1:3κ²*S*; 2:3κ²*S*-tris(tricyclohexylphosphine)-1κ*P*,2κ*P*,3κ*P*-*triangulo*-triplatinum–benzene (1/0.5).

Supplementary data available: see Instructions for Authors, *J. Chem. Soc., Dalton Trans.*, 1990, Issue 1, pp. xix—xxii.

Table 1. Chemical shifts (p.p.m.) and coupling constants (Hz) for $[Pt_3(\mu\text{-}CO)_{3-n}(\mu\text{-}SO_2)_n\{P(C_6H_{11})_3\}_3]$ and $[Pt_2(\mu\text{-}SO_2)(CO)_2\{P(C_6H_{11})_3\}_2]$

			P^2	P^3	Pt^1	Pt^2	Pt^3
$[Pt_3(\mu\text{-}SO_2)_3\{P(C_6H_{11})_3\}_3]$							
$\delta(^{31}P)$	76.3	P^1	49	49	3 760	330	330
		P^2		49	330	3 760	330
$\delta(^{195}Pt)$	−4 070	P^3			330	330	3 760
		Pt^1				700	700
		Pt^2					700
$[Pt_3(\mu\text{-}CO)(\mu\text{-}SO_2)_2\{P(C_6H_{11})_3\}_3]$							
$\delta(^{31}P^{1,2})$	77.4	P^1	49	53	3 959	280	347
$\delta(^{31}P^3)$	57.9	P^2		53	280	3 959	347
		P^3			337	337	3 889
$\delta(^{195}Pt^{1,2})$	−4 165	Pt^1				*a*	600
$\delta(^{195}Pt^3)$	−3 570	Pt^2					600
$[Pt_3(\mu\text{-}CO)_2(\mu\text{-}SO_2)\{P(C_6H_{11})_3\}_3]$							
$\delta(^{31}P^1)$	82.2	P^1	51	51	5 134	449	449
$\delta(^{31}P^{2,3})$	61.9	P^2		62	372	4 055	301
		P^3			372	301	4 055
$\delta(^{195}Pt^1)$	−4 011	Pt^1				1 830	1 830
$\delta(^{195}Pt^{2,3})$	−4 515	Pt^2					*a*
$[Pt_3(\mu\text{-}SO_2)_3\{P(C_6H_{11})_3\}_3]$							
$\delta(^{31}P)$	68.8	P^1	60	60	4 410	426	426
		P^2		60	426	4 410	426
$\delta(^{195}Pt)$	−4 392	P^3			426	426	4 410
		Pt^1				1 560	1 560
		Pt^2					1 560
$[Pt_2(\mu\text{-}SO_2)(CO)_2\{P(C_6H_{11})_3\}_2]$							
$\delta(^{31}P)$	29.2	P^1	67		3 800	284	
		P^2			284	3 800	
		Pt^1				*b*	

[a] Coupling constant could not be measured from the spectrum. [b] Coupling constant could not be obtained from $^{31}P\text{-}\{^1H\}$ spectrum.

Table 2. Infrared data for $[Pt_3(\mu\text{-}CO)_{3-n}(\mu\text{-}SO_2)_n\{P(C_6H_{11})_3\}_3]$ and $[Pt_2(\mu\text{-}SO_2)(CO)_2\{P(C_6H_{11})_3\}_2]$

	$\nu(CO)/cm^{-1}$	$\nu(SO_2)/cm^{-1}$
$[Pt_3(SO_2)_3\{P(C_6H_{11})_3\}_3]$	—	1 245m, 1 081s
$[Pt_3(CO)(SO_2)_2\{P(C_6H_{11})_3\}_3]$	1 840vs	1 234m, 1 080s, 1 071vs
$[Pt_3(CO)_2(SO_2)\{P(C_6H_{11})_3\}_3]$	1 847m, 1 784vs	1 206w, 1 070s
$[Pt_3(CO)_3\{P(C_6H_{11})_3\}_3]$	1 770vs, 1 737w	—
$[Pt_2(SO_2)(CO)_2\{P(C_6H_{11})_3\}_2]$	2 032s, 1 994w	1 022m

quantities are specified, *e.g.* 1 equivalent of CO, the reactions were performed in a quantitative fashion using a high-vacuum line. The mode of addition can make a considerable difference to the course of the reaction. For instance, when 1 equivalent of CO gas is added to $[Pt_3(\mu\text{-}SO_2)_3\{P(C_6H_{11})_3\}_3]$ (**1**) either in CH_2Cl_2 at −78 or benzene at 20 °C the monosubstituted cluster $[Pt_3(\mu\text{-}CO)(\mu\text{-}SO_2)_2\{P(C_6H_{11})_3\}_3]$ (**2**) is obtained in high yield. In contrast, when CO gas is bubbled through the CH_2Cl_2 solution at the same temperatures for ⩾10 s the dimeric product $[Pt_2(\mu\text{-}SO_2)(CO)_2\{P(C_6H_{11})_3\}_2]$ (**3**) is isolated.

The disubstituted product $[Pt_3(\mu\text{-}CO)_2(\mu\text{-}SO_2)\{P(C_6H_{11})_3\}_3]$ (**4**) was isolated in high yield either by adding 1 equivalent of CO to (**2**) in benzene or by passing CO through a solution of (**1**) in benzene at 60 °C. It can be converted into the monosubstituted (**2**) and the parent SO_2 compound (**1**) by the

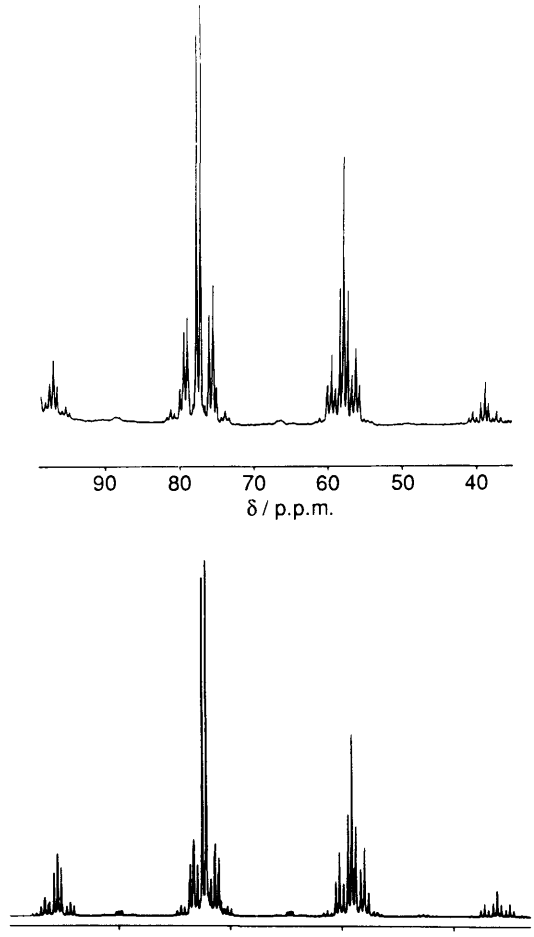

Figure 1. Observed (top) and simulated (bottom) $^{31}P\text{-}\{^1H\}$ n.m.r. spectra of $[Pt_3(\mu\text{-}CO)(\mu\text{-}SO_2)_2\{P(C_6H_{11})_3\}_3]$ (**2**)

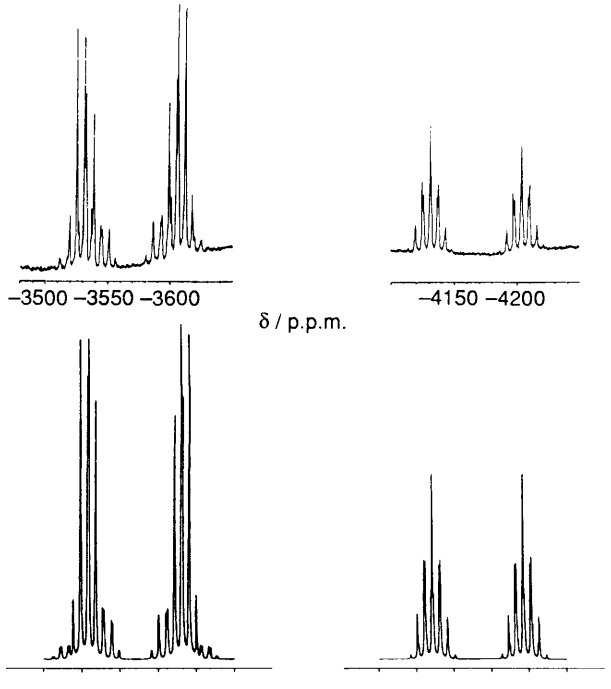

Figure 2. Observed (top) and simulated (bottom) $^{195}Pt\text{-}\{^1H\}$ n.m.r. spectra of compound (**2**)

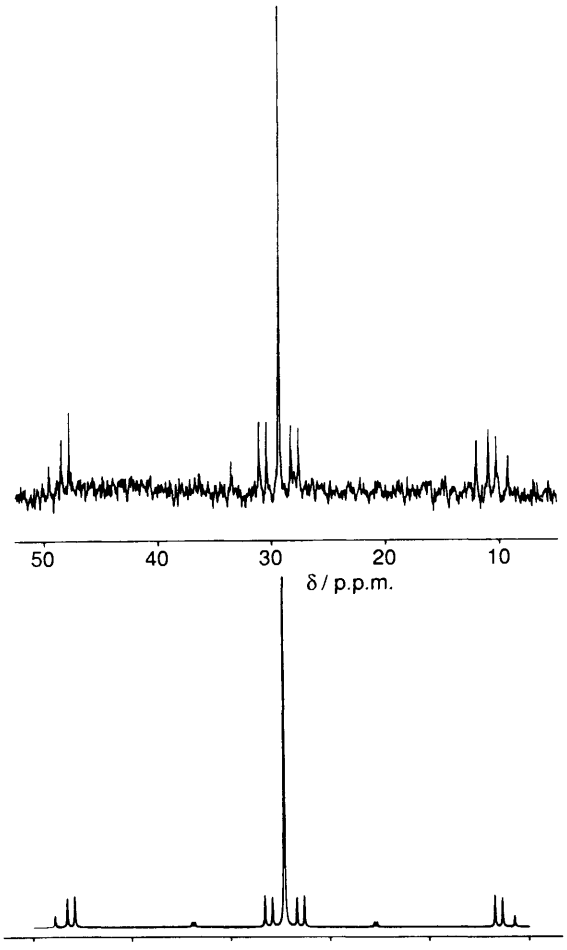

Figure 3. Observed (top) and simulated (bottom) ^{31}P-$\{^1H\}$ n.m.r. spectra of $[Pt_2(\mu\text{-}SO_2)(CO)_2\{P(C_6H_{11})_3\}_3]$ (**3**)

Table 3. Crystal data for compound (**2**)

Formula	$C_{55}H_{99}O_5P_3Pt_3S_2 \cdot 0.5C_6H_6$
M	1 582.43 (1 621.48 including 0.5 benzene)
Crystal system	Monoclinic
Space group	$C2/m$
a/Å	24.909(9)
b/Å	21.694(4)
c/Å	15.559(9)
β/°	125.41(3)
U/Å^3	6 852.19
Z	4
D_c/g cm^{-3}	1.572
F(000)	3 204
Linear absorption coefficient/cm^{-1}	63.7356
Crystal colour	Yellow
Data collection	
X-radiation	Mo-K_α, λ = 0.710 69 Å
$\theta_{min.}$, $\theta_{max.}$/°	1, 25
minimum, maximum h, k, l	−1, 29; −1, 25; −18, 18
ω-scan width/°	1.35 + 0.35 tan θ
horizontal aperture/mm	4
total data collected	7 971
total unique data	6 192
total observed data [$I > 3\sigma(I)$]	4 549
Merging R factor	0.022
Absorption correction	ψ-Scan profile; minimum, maximum correction 0.99, 1.80

successive addition of 1 equivalent of SO_2. The tricarbonyl cluster $[Pt_3(\mu\text{-}CO)_3\{P(C_6H_{11})_3\}_3]$ (**5**) cannot be obtained directly from (**4**) and CO gas. The reaction can, however, be facilitated by adding Me_3NO.[11] Addition of Me_3NO to a solution of compound (**4**) in benzene at room temperature led to the formation of (**5**) in high yield (>90%). The extent of acceleration of the rate of reaction depended on the mole ratio of Me_3NO: 3 equivalents required a reaction time of 6—8 h and 20 equivalents required 2—3 h. The reaction was reversed when 1 equivalent of SO_2 was added to (**5**), but when SO_2 was passed through a solution of (**5**) at room temperature the dimer (**3**) was formed as the major product and (**4**) as the minor product.

Spectroscopic Characterisation of the Compounds.—The compounds were characterised on the basis of ^{31}P-$\{^1H\}$ and ^{195}Pt-$\{^1H\}$ n.m.r. and i.r. spectroscopic data. The former are summarised in Table 1 and the latter in Table 2. The fully substituted cluster $[Pt_3(\mu\text{-}CO)_3\{P(C_6H_{11})_3\}_3]$ (**5**) has a strong ν(CO) band at 1 770 cm^{-1} which is associated with the e' mode for the bridging carbonyls in this D_{3h} structure. In the lower-symmetry clusters $[Pt_3(\mu\text{-}CO)_2(\mu\text{-}SO_2)\{P(C_6H_{11})_3\}_3]$ (**4**) and $[Pt_3(\mu\text{-}CO)(\mu\text{-}SO_2)_2\{P(C_6H_{11})_3\}_3]$ (**2**) this is replaced by bands at 1 847 and 1 784, and 1 840 cm^{-1} respectively. The overall shift to higher frequencies suggests that the bridging SO_2 ligand is acting as a better π-acceptor ligand. The corresponding ν(SO_2) frequencies given in Table 2 lend support to this interpretation.

The ^{31}P-$\{^1H\}$ and ^{195}Pt-$\{^1H\}$ n.m.r. spectra for compound (**2**) are shown in Figures 1 and 2 and were satisfactorily simulated using the following spin systems: ^{31}P-$\{^1H\}$, A_2B (29.1%, no ^{195}Pt nuclei); A_2BX (14.8%, one ^{195}Pt nucleus in the unique position); AA′BY (29.6%, one ^{195}Pt nucleus in one of the symmetry-related positions); AA′BXY (15.1%, two ^{195}Pt nuclei in symmetry-inequivalent positions); AA′BXX′ (7.5%, two ^{195}Pt nuclei in symmetry-equivalent positions); and AA′BXX′Y (3.8%, three ^{195}Pt nuclei). The relevant parameters obtained from the computer simulations are given in Table 1.

The ^{31}P-$\{^1H\}$ n.m.r. data for the dimeric compound $[Pt_2(\mu\text{-}SO_2)(CO)_2\{P(C_6H_{11})_3\}_2]$ (**3**) were simulated using the following spin systems: A_2 (44.0%, no ^{195}Pt nuclei); AA′X (44.7%, one ^{195}Pt nucleus), and AA′XX′ (11.4%, two ^{195}Pt nuclei). The relevant observed and computed spectra, which are characteristic for a dimeric platinum cluster with a linear P–Pt–Pt–P skeleton, are illustrated in Figure 3 and the coupling constants summarised in Table 1. The coupling constants for this compound are similar to those reported previously for $[Pt_2(\mu\text{-}SO_2)(CO)_2(PBu^t{}_2Ph)_2]$.

The n.m.r. parameters for (**2**) and (**4**) have been compared with those for the symmetrical triangular clusters (**1**) and (**5**) in Table 1. The chemical shifts and coupling constants do not show clear trends which can be readily interpreted in terms of the substitutional patterns. Indeed, ^1J(Pt–Pt) appears to be the only reliable guide to the substitutional patterns since it is observed at 250—700 Hz for bonds bridged by SO_2 and 1 300—1 830 Hz for bonds bridged by CO.

X-*Ray Crystallographic Analysis.*—The structure of compound (**2**) was confirmed by a single-crystal X-ray crystallographic investigation (details of which are given in Table 3) and the results of which are summarised in Tables 4 and 5. The important structural features of the platinum triangle are illustrated in Figure 4. The triangular cluster lies on a crystallographically imposed mirror plane of symmetry. The platinum atoms define an isosceles triangle with Pt–Pt distances of 2.710(1) Å bridged by SO_2 and 2.678(1) Å bridged by CO. These are substantially shorter than those reported for the symmetrical SO_2 cluster $[Pt_3(\mu\text{-}SO_2)_3\{P(C_6H_{11})_3\}_3]$[12] (**1**), 2.814(1) Å, but only slightly longer than those reported for $[Pt_3(\mu\text{-}CO)_3$-

Table 4. Important bond lengths (Å) and angles (°) for compound (**2**)

Pt(1)–Pt(2)	2.710(1)	Pt(2)–C(1)	2.218(6)
Pt(2)–Pt(2′)	2.678(1)	P(1)–C(2)	1.85(1)
Pt(1)–P(1)	2.300(3)	P(1)–C(6)	1.857(9)
Pt(2)–P(2)	2.308(2)	S(1)–O(1)	1.33(1)
Pt(1)–S(1)	2.280(3)	S(1)–O(2)	1.46(1)
Pt(2)–S(1)	2.264(3)	C(1)–O(3)	1.11(2)
Pt(2)–Pt(1)–Pt(2′)	59.22(2)	C(1)–Pt(2)–Pt(2′)	52.9(1)
Pt(1)–Pt(2)–Pt(2′)	60.39(1)	Pt(1)–P(1)–C(2)	112.1(4)
Pt(2)–Pt(1)–P(1)	150.33(1)	Pt(2)–P(2)–C(18)	111.0(6)
P(1)–Pt(2)–Pt(2′)	148.36(6)	C(1)–Pt(2)–S(1)	97.2(1)
Pt(2)–Pt(1)–S(1)	112.28(7)	Pt(1)–S(1)–O(1)	117.1(5)
Pt(2)–Pt(1)–S(1′)	53.10(7)	Pt(2)–S(1)–O(2)	115.2(4)
Pt(1)–S(1)–Pt(2)	73.2(1)	O(3)–C(1)–Pt(2)	103.9(3)
Pt(1)–Pt(2)–C(1)	111.8(1)	C(2)–P(1)–C(6)	133.2(7)
Pt(2)–C(1)–Pt(2′)	74.3(2)	O(1)–S(2)–O(2)	133.2(7)

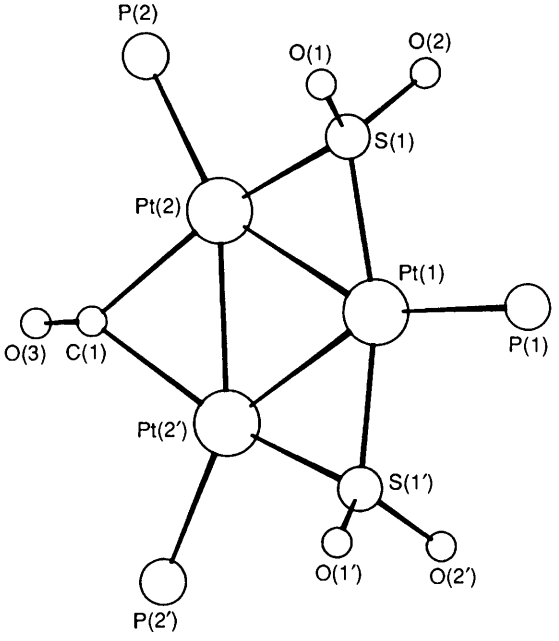

Figure 4. Molecular structure of $[Pt_3(\mu\text{-}CO)(\mu\text{-}SO_2)_2\{P(C_6H_{11})_3\}_3]$ (**2**). For reasons of clarity the cyclohexyl rings have been omitted. The cluster has a crystallographically imposed plane of symmetry which passes through P(1), Pt(1), C(1), and O(3)

$\{P(C_6H_{11})_3\}_3]$[13] (**5**), 2.655(2) Å. The longer distance in the former has been attributed to steric effects between the SO_2 ligands. Presumably, in the disubstituted derivative (**2**), these repulsive interactions are less pronounced and consequently Pt–Pt bond lengths resemble those of the carbonyl cluster (**5**) more closely.

Stopped-flow Infrared Studies.—In order to gain a better insight into these reactions, some stopped-flow i.r. studies were undertaken in collaboration with Dr. J. Maher.[14] A dichloromethane solution of $[Pt_3(\mu\text{-}SO_2)_3\{P(C_6H_{11})_3\}_3]$ (**1**) was mixed with a CO-saturated dichloromethane solution. This showed the presence of the dimer (**3**), identified by the band of 2 038 cm^{-1} in the first spectrum, recorded 0.36 s after mixing. The rate of dimer formation is remarkably fast, and underlines the ease with which cluster degradation and aggregation reactions can occur. The dimer is slowly converted into (**4**). Some compound (**2**) is also produced in this reaction. No evidence was obtained for the proposed intermediate $[Pt_3(\mu\text{-}SO_2)_3(CO)\{P(C_6H_{11})_3\}_3]$, but the presence of the dimer in the first recorded spectrum is consistent with the rapid formation and decomposition of this species.

Table 5. Positional parameters (× 10^4) for compound (**2**) with estimated standard deviations in parentheses

Atom	*X/a*	*Y/b*	*Z/c*
Pt(1)*	3 343(2)	0	409(3)
Pt(2)	2 589(2)	−617(2)	−1 442(2)
P(1)	4 108(1)	0	2 210(2)
P(2)	2 281(1)	−1 525(1)	−2 389(2)
S(1)	3 224(2)	1 042(1)	186(2)
O(1)	2 929(6)	1 331(4)	566(6)
O(2)	3 801(5)	1 377(4)	415(7)
O(3)	1 646(8)	0	−3 613(10)
C(1)	1 873(4)	0	−2 753(5)
C(2)	3 718(5)	0	2 920(9)
C(3)	3 319(5)	−583(5)	2 723(9)
C(4)	3 032(5)	−571(5)	3 361(8)
C(5)	2 620(8)	0	3 123(12)
C(6)	4 626(4)	705(4)	2 694(7)
C(7)	5 038(6)	781(6)	2 261(12)
C(8)	5 344(6)	1 413(6)	2 503(11)
C(9)	5 755(6)	1 533(6)	3 665(13)
C(10)	5 366(7)	1 433(7)	4 128(9)
C(11)	5 053(6)	810(6)	3 883(7)
C(12)	2 891(4)	−2 146(5)	−1 692(8)
C(13)	3 511(5)	2 019(5)	−1 637(9)
C(14)	4 061(6)	−2 481(7)	−871(12)
C(15)	3 839(7)	−3 144(7)	−1 165(12)
C(16)	3 224(6)	−3 164(6)	−1 253(10)
C(17)	2 672(6)	−2 821(5)	2 026(10)
C(18)	2 089(4)	−1 407(5)	−3 719(7)
C(19)	2 640(5)	−1 040(5)	−3 692(7)
C(20)	2 390(5)	−850(5)	−4 812(8)
C(21)	2 180(6)	−1 410(6)	−5 527(8)
C(22)	1 663(6)	−1 783(6)	−5 527(8)
C(23)	1 896(6)	−1 967(5)	−4 418(8)
C(24)	1 515(4)	−1 844(5)	−2 655(7)
C(25)	931(5)	−1 425(6)	−3 321(10)
C(26)	298(5)	−1 708(8)	−3 511(11)
C(27)	386(6)	−1 880(7)	−2 514(11)
C(28)	966(6)	−2 287(7)	−1 838(10)
C(29)	1 592(5)	−1 991(5)	−1 619(8)
C(100)	5 615(6)	297(5)	626(9)
C(101)	5 000	637(9)	0

* The atoms Pt(1), P(1), O(3), C(1), C(2), and C(5) lie on the mirror plane. Carbon atoms C(2), C(3), C(4), and C(5) are associated with the cyclohexyl ring attached to P(1) and lying perpendicular to the mirror plane. The second symmetry-independent cyclohexyl ring attached to this phosphorus is defined by C(6)–C(11). The atom sequences C(12)–C(17), C(18)–C(23), and C(24)–C(29) are the carbon atoms associated with the cyclohexyl rings bonded to P(2). Carbon atoms C(100) and C(101) are associated with the benzene of solvation.

Reactions of $[Pt_3(\mu\text{-}CO)(\mu\text{-}SO_2)_2\{P(C_6H_{11})_3\}_3]$ (**2**) *and* $[Pt_3(\mu\text{-}CO)_2(\mu\text{-}SO_2)\{P(C_6H_{11})_3\}_3]$ (**4**) *with Xylyl Isocyanide.*—We have previously reported the reactions of $[Pt_3(\mu\text{-}CO)_3\{P(C_6H_{11})_3\}_3]$[2] and $[Pt_3(\mu\text{-}SO_2)_3\{P(C_6H_{11})_3\}_3]$[15] with xylyl isocyanide. In the former case CO and $P(C_6H_{11})_3$ substitution occurs to give $[Pt_3(\mu\text{-}CO)(\mu\text{-}CNR)_2(CNR)\{P(C_6H_{11})_3\}_2]$ (R = C_8H_9) and $[Pt_3(\mu\text{-}CNR)_3(CNR)_2\{P(C_6H_{11})_3\}]$ as the exclusive products, whereas in the latter case $[Pt_3(\mu\text{-}SO_2)_2(CNR)_2\{P(C_6H_{11})_3\}_3]$ (**6**) is formed when 2 equivalents of isocyanide are used, and the dimer $[Pt_2(\mu\text{-}SO_2)(CNR)_2\{P(C_6H_{11})_3\}_2]$ (**7**) when ⩾3 equivalents are used. Therefore, it was of interest to establish how the intermediate and less-symmetric clusters (**2**) and (**4**) reacted with the same isocyanide. The relevant reaction products are summarised in Scheme 3.

The reaction pathways observed for $[Pt_3(\mu\text{-}CO)_{3-n}(\mu\text{-}SO_2)_n$-

$\{P(C_6H_{11})_3\}_3$] are dominated by the presence of SO_2 since $[Pt_3(\mu\text{-}SO_2)_3\{P(C_6H_{11})_3\}_3]$, $[Pt_3(\mu\text{-}CO)(\mu\text{-}SO_2)_2\{P(C_6H_{11})_3\}_3]$, and $[Pt_3(\mu\text{-}CO)_2(\mu\text{-}SO_2)\{P(C_6H_{11})_3\}_3]$ give the same dimeric compound $[Pt_2(\mu\text{-}SO_2)(CNR)_2\{P(C_6H_{11})_3\}_2]$ with 3 equivalents of CNC_8H_9, and show no evidence of the phosphine-substitution reactions described previously for $[Pt_3(\mu\text{-}CO)_3\{P(C_6H_{11})_3\}_3]$. For all of the compounds $[Pt_3(\mu\text{-}CO)_{3-n}(\mu\text{-}SO_2)_n\{P(C_6H_{11})_3\}_3]$ the initial intermediate with isocyanide is likely to be the 44-electron addition product (**8**). When X = X′ = X″ = CO the isocyanide can displace a bridging CO and terminal phosphine by the concerted process in Scheme 4. However, when X, X′, or X″ is SO_2 this process does not appear to be favourable since we have never seen evidence for bridging isocyanides when SO_2 is present. When X = X′ = X″ = SO_2 or X = X′ = SO_2 and X″ = CO compound (**8**) appears to react with a further equivalent of isocyanide with the displacement of the X″ ligand to give (**6**). This process cannot occur when X = X″ = CO and cluster fragmentation results to give (**7**). The cluster (**6**) also appears to be susceptible to fragmentation since it reacts with a further equivalent of CNC_8H_9 to give (**7**).

The reactions described in this paper underline the fine balance which can occur between addition, substitution, and fragmentation reactions of triangular platinum cluster compounds.

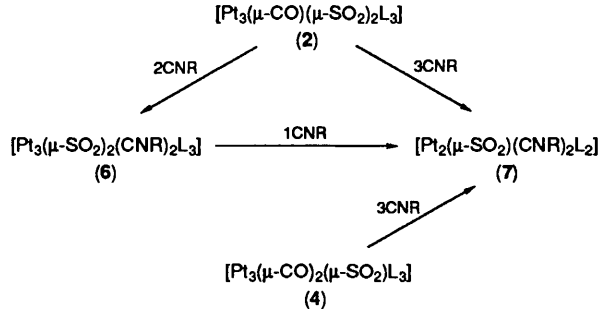

Scheme 3. L = $P(C_6H_{11})_3$, R = C_8H_9

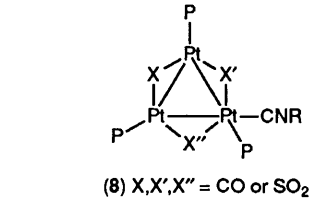

(**8**) X,X′,X″ = CO or SO_2

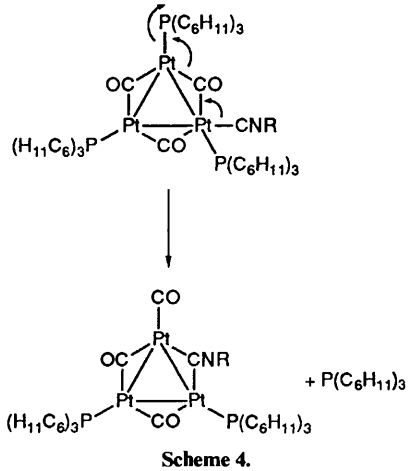

Scheme 4.

Experimental

Reactions were routinely carried out using Schlenk-line techniques under pure dry dinitrogen, with dry oxygen-free solvents. Microanalyses (N, C, and H) were carried out by Mr. M. Gascoyne and his staff at this laboratory. Infrared spectra were recorded on a Perkin-Elmer FT1710 spectrometer and a Mattson Polaris spectrometer as Nujol mulls between KBr or CsI discs, or as solutions in KBr cells. The $^{31}P\text{-}\{^1H\}$ and $^{195}Pt\text{-}\{^1H\}$ n.m.r. spectra were run using a Bruker AM 250 spectrometer, using $P(OMe)_3O$ in D_2O and Na_2PtCl_6 in D_2O respectively as references. The machine operating frequencies were 101.26 MHz for ^{31}P and 53.57 MHz for ^{195}Pt. N.m.r. simulations were carried out using the Oxford University VAX system using a program developed by Professor R. K. Harris and adapted for use at Oxford by Dr. A. E. Derome.

The compound $[Pt_3(\mu\text{-}CO)_3\{P(C_6H_{11})_3\}_3]\cdot C_6H_6$ (**5**) was synthesised using the method of Clark *et al.*[16]

Syntheses.—$[Pt_3(\mu\text{-}SO_2)_3\{P(C_6H_{11})_3\}_3]$ (**1**). Compound (**5**) (0.50 g, 0.32 mmol) was dissolved in benzene (60 cm^3) and the solution warmed to 60 °C. Sulphur dioxide gas was bubbled through the solution for 45 min. Concentration of the solution followed by addition of hexane led to the precipitation of orange microcrystals. Yield 0.45 g (88%) (Found: C, 40.2; H, 6.2. $C_{54}H_{99}O_6P_3Pt_3S_3\cdot C_6H_6$ requires C, 40.0; H, 6.1%).

$[Pt_3(\mu\text{-}CO)(\mu\text{-}SO_2)_2\{P(C_6H_{11})_3\}_3]$ (**2**). (*i*) Compound (**1**) (0.30 g, 0.19 mmol) was dissolved in benzene (80 cm^3), and the solution was frozen in liquid nitrogen and then evacuated. Using a high-vacuum line 1 equivalent of CO was added, and the reaction mixture allowed to warm to room temperature. The orange solution was concentrated *in vacuo* and methanol added to yield 0.23 g (78%) of compound (**2**) as yellow microcrystals (Found: C, 43.0; H, 6.6. $C_{55}H_{99}O_5P_3Pt_3S_2\cdot 0.5C_6H_6$ requires C, 43.0; H, 6.3%).

(*ii*) Compound (**4**) (0.12 g, 0.07 mmol) was dissolved in benzene (20 cm^3), frozen in liquid nitrogen, and then evacuated. To this was added 1 equivalent of SO_2 gas, and the reaction mixture allowed to warm to room temperature. After stirring for 5 min the solvent was removed *in vacuo* and the solid recrystallised from CH_2Cl_2–methanol.

$[Pt_3(\mu\text{-}CO)_2(\mu\text{-}SO_2)\{P(C_6H_{11})_3\}_3]$ (**4**). (*i*) Compound (**1**) (0.63 g, 0.39 mmol) was dissolved in benzene (50 cm^3) and CO gas bubbled through the solution for 10 min at 60 °C to form a yellow solution. The solvent was removed *in vacuo*, and the solid recrystallised from benzene–ethanol to give 0.46 g (77%) of yellow crystals (Found: C, 43.7; H, 6.5. $C_{56}H_{99}O_4P_3Pt_3S$ requires C, 43.5; H, 6.4%).

(*ii*) Compound (**2**) (0.20 g, 0.13 mmol) was dissolved in benzene (20 cm^3), frozen in liquid nitrogen, and then evacuated. One equivalent of CO gas was then added, and the reaction mixture allowed to warm to room temperature and stirred for 5 min. The solvent was then removed *in vacuo*, and the solid recrystallised from CH_2Cl_2–methanol. Yield 0.18 g (90%).

(*iii*) Compound (**5**) (0.20 g, 0.13 mmol) was dissolved in benzene (20 cm^3), frozen in liquid nitrogen, and then evacuated. One equivalent of SO_2 gas was added, and the reaction mixture allowed to warm to room temperature then stirred for 5 min. The solvent was removed *in vacuo* and the solid recrystallised from CH_2Cl_2–methanol. Yield 0.18 g (90%).

$[Pt_2(\mu\text{-}SO_2)(CO)_2\{P(C_6H_{11})_3\}_2]$ (**3**). (*i*) Compound (**1**) (0.05 g, 0.031 mmol) was dissolved in dichloromethane (20 cm^3), and cooled to −78 °C. Carbon monoxide gas was passed through the orange-red solution for 10 s, causing an immediate colour change to pale yellow. The solution was stirred for 30 min and then taken to dryness. Recrystallisation from CH_2Cl_2–hexane gave a yellow microcrystalline solid.

(*ii*) Compound (**5**) (0.20 g, 0.13 mmol) was dissolved in benzene (20 cm^3) and SO_2 gas bubbled through the solution for

1 min at room temperature giving a pale yellow solution. The solvent was removed *in vacuo* giving a yellow powder.

Reactions with CNC_8H_9.—*Synthesis of* $[Pt_3(\mu\text{-}SO_2)_2(CNC_8H_9)_2\{P(C_6H_{11})_3\}_3]$ (**6**). A solution of CNC_8H_9 (0.0163 g, 0.12 mmol) in benzene (20 cm^3) was added to compound (**2**) (0.100 g, 0.062 mmol) in benzene (30 cm^3). This gave an immediate colour change from yellow to red. The mixture was stirred for 30 min, the resultant solution taken to dryness, and the solid recrystallised from benzene–acetonitrile. Yield 0.084 g (73%) (Found: C, 46.0; H, 6.4; N, 1.6. $C_{72}H_{117}N_2O_4P_3Pt_3S_2$ requires C, 46.1; H, 6.3; N, 1.6%). ν(CN) 2 111s, ν(SO_2) 1 261m and 1 023s cm^{-1}. N.m.r. data: δ(^{31}P) 38.2 and 26.0; δ(^{195}Pt) −4 861 and −5 472 p.p.m.; ^1J(Pt–Pt) 920, ^1J(Pt–Pt′) 697, ^1J(Pt–P) 4 951, ^1J(Pt–P′) 4 296, ^2J(Pt–P) 241, ^3J(P–P) 55, and ^3J(P–P) 38 Hz.

Synthesis of $[Pt_2(\mu\text{-}SO_2)(CNC_8H_9)_2\{P(C_6H_{11})_3\}_2]$ (**7**). (*i*) A solution of CNC_8H_9 (0.0249 g, 0.19 mmol) in benzene (20 cm^3) was added to compound (**2**) (0.100 g, 0.062 mmol) in benzene (30 cm^3). The solution immediately darkened. Stirring was continued for 30 min and the resultant orange solution taken to dryness, the product washed with diethyl ether and recrystallised from CH_2Cl_2–methanol. Yield. 0.077 g (63%) (Found: C, 49.4; H, 7.0; N, 1.9. $C_{54}H_{84}N_2O_2P_2Pt_2S$ requires C, 49.6; H, 6.5; N, 2.1%). ν(CN) 2 117vs and 2 081 (sh); ν(SO_2) 1 152m and 1 021s cm^{-1}. N.m.r. data: δ(^{31}P) 25.9 p.p.m., δ(^{195}Pt) −5 258 p.p.m., ^1J(Pt–Pt) 920, ^1J(Pt–P) 3 624, ^2J(Pt–P) 375, and ^3J(P–P) 91 Hz.

(*ii*) A solution of CNC_8H_9 (0.0253 g, 0.19 mmol) in benzene (20 cm^3) was added to compound (**4**) (0.100 g, 0.064 mmol) in benzene (30 cm^3). Stirring was continued for 30 min, and the resultant orange solution was taken to dryness. The solid was recrystallised from CH_2Cl_2–methanol giving yellow microcrystals. Yield 0.087 g (75%).

Attempted synthesis of $[Pt_3(\mu\text{-}CO)(\mu\text{-}SO_2)(CNC_8H_9)_2\{P(C_6H_{11})_3\}_3]$. A solution of CNC_8H_9 (0.017 g, 0.13 mmol) in benzene (20 cm^3) was added to compound (**4**) (0.100 g, 0.065 mmol) in benzene (30 cm^3). The mixture was stirred for 30 min, and the resultant orange solution taken to dryness *in vacuo*. ν(CN) 2 117s and 2 081 (sh); ν(SO_2) 1 152m, 1 066s, and 1 021s cm^{-1}. ^{31}P-{^{1}H} n.m.r. data; δ 82.3(t), 62.0 (d), and 26.0 (m) p.p.m. consistent with a mixture of compounds (**4**) and (**7**).

Crystal Structure Determination of $[Pt_3(\mu\text{-}CO)(\mu\text{-}SO_2)_2\{P(C_6H_{11})_3\}_3]$ (**2**).— Crystals of compound (**2**) used in the analysis were grown from a slow diffusion of methanol into a benzene solution. A single crystal of dimensions 0.05 × 0.08 × 0.15 mm was mounted in a glass capillary and transferred to the goniometer head of an Enraf-Nonius CAD-4 diffractometer. The experimental details associated with the crystallographic determination are summarised in Table 3. The data were corrected for Lorentz and polarisation effects as well as absorption (maximum, minimum correction 1.8, 0.99). There were no significant changes in the intensities of the standard reflections.

The structure was solved by routine Patterson and Fourier methods and refinement was effected through full-matrix least-squares methods, anisotropic thermal parameters being assigned to all non-hydrogen atoms. The hydrogens were generated geometrically and were not refined. The molecule (**2**) has a crystallographically imposed mirror plane of symmetry and the atoms Pt(1), P(1), O(3), C(1), C(2), and C(5) all lie on this plane. A Chebyshev weighting scheme with coefficients 9.48, −2.12, and 7.18 gave satisfactory agreement analyses; R and R' values were 0.046 and 0.054 respectively. Programs and scattering factors used are given in refs. 17 and 18.

Additional material available from the Cambridge Crystallographic Data Centre comprises H-atom co-ordinates, thermal parameters, and remaining bond lengths and angles.

Acknowledgements

The S.E.R.C. is thanked for financial support, Johnson-Matthey for generous loans of platinum, and Dr. John Maher for carrying out the stopped-flow experiments.

References

1 D. M. P. Mingos and R. W. M. Wardle, *Transition. Met. Chem. (Weinheim, Ger.)*, 1985, **10**, 441.
2 C. E. Briant, D. I. Gilmour, D. M. P. Mingos, and R. W. M. Wardle, *J. Chem. Soc., Dalton Trans.*, 1985, 1693.
3 G. Douglas, L. Manojlovic-Muir, K. W. Muir, M. Rashidi, C. M. Anderson, and R. J. Puddephatt, *J. Am. Chem. Soc.*, 1987, **109**, 6527.
4 C. Couture, D. H. Farrar, D. S. Fisher, and R. R. Gukathasan, *Organometallics*, 1987, **6**, 532.
5 C. E. Briant, R. W. M. Wardle, and D. M. P. Mingos, *J. Organomet. Chem.*, 1984, **267**, C49.
6 D. M. P. Mingos, P. Oster, and D. J. Sherman, *J. Organomet. Chem.*, 1987, **320**, 257.
7 A. Albinati, K-H. Dahman, A. Togni, and L. M. Venanzi, *Angew. Chem., Int. Ed. Engl.*, 1985, **24**, 766.
8 C. S. Browning, D. H. Farrar, R. R. Gukathasan, and S. A. Morris, *Organometallics*, 1985, **4**, 1750.
9 A. Albinati, G. Carturan, and A. Musco, *Inorg. Chim. Acta*, 1976, **16**, L3.
10 M. F. Hallam, N. D. Howells, D. M. P. Mingos, and R. W. M. Wardle, *J. Chem. Soc., Dalton Trans.*, 1985, 845.
11 M. F. Hallam and D. M. P. Mingos, *J. Organomet. Chem.*, 1986, **315**, C35.
12 S. G. Bott, M. F. Hallam, O. J. Ezomo, D. M. P. Mingos, and I. D. Williams, *J. Chem. Soc., Dalton Trans.*, 1988, 1461.
13 A. Albinati, *Inorg. Chim. Acta*, 1977, **22**, L31.
14 J. Maher, University of Bristol, unpublished work.
15 D. M. P. Mingos, I. D. Williams, and M. J. Watson, *J. Chem. Soc., Dalton Trans.*, 1988, 1509.
16 H. C. Clark, A. B. Goel, and C. S. Wong, *Inorg. Chim. Acta*, 1979, **34**, 159.
17 D. J. Watkin, J. R. Carruthers, and P. W. Retteridge, CRYSTALS User Manual, Chemical Crystallography Laboratory, University of Oxford, 1985.
18 'International Tables for *X*-Ray Crystallography,' Kynoch Press, Birmingham, 1974.

Received 14*th March* 1990; *Paper* 0/01131B